

Multiwavelength Spectral Models for SNR G347.3-0.5 from Non-Linear Shock Acceleration

Matthew G. Baring^a, Donald C. Ellison^b, and Patrick O. Slane^c

^a*Department of Physics and Astronomy, MS-108, Rice University, P. O. Box 1892, Houston, TX 77251-1892, USA, Email: baring@rice.edu*

^b*Department of Physics, North Carolina State University, Box 8202, Raleigh, NC 27695, USA, Email: don_ellison@ncsu.edu*

^c*Harvard-Smithsonian Center for Astrophysics, 60 Garden Street, Cambridge, MA 02138, USA, Email: slane@head.cfa.harvard.edu*

Abstract

The remnant G347.3-0.5 exhibits strong shell emission in the radio and X-ray bands, and has a purported detection in the TeV gamma-ray band by the CANGAROO-II telescope. The CANGAROO results were touted as evidence for the production of cosmic ray ions, a claim that has proven controversial due to constraining fluxes associated with a proximate unidentified EGRET source 3EG J1714-3857. HESS has now seen this source in the TeV band. The complex environment of the remnant renders modeling of its broadband spectrum sensitive to assumptions concerning the nature and parameters of the circumremnant medium. This paper explores a sampling of reasonable possibilities for multiwavelength spectral predictions from this source, using a non-linear model of diffusive particle acceleration at the shocked shell. The magnetic field strength, shell size and degree of particle cross-field diffusion act as variables to which the radio to X-ray to gamma-ray signal is sensitive. The modeling of the extant data constrains these variables, and the potential impact of the recent HESS detection on such parameters is addressed. Putative pion decay signals in hard gamma-rays resulting from hadronic interactions in dense molecular clouds are briefly discussed; the requisite suppression of the GeV component needed to accommodate the 3EG J1714-3857 EGRET data provides potential bounds on the diffusive distance from the shell to the proximate clouds.

Key words:

Supernova Remnants, Shock Acceleration, Cosmic Rays, Inverse Compton Scattering, Synchrotron Radiation, Imaging Atmospheric Čerenkov Telescopes

1 Introduction

Supernova remnants (SNRs) are believed to be the principal candidates for generating galactic cosmic rays, relativistic ions and electrons with energies from the GeV range up to 10^{15} eV and beyond. A Holy Grail of cosmic ray physics has been to secure a radiative detection that would unambiguously indicate the presence of cosmic ray ions in proximity to one or more supernova remnants, thereby establishing a direct connection between source and diffuse population. The search has therefore focused on gamma-ray emission signaling the decay of neutral pions, $\pi^0 \rightarrow \gamma\gamma$; these are presumably generated in collisions between cosmic ray protons accelerated at the shocked outer shells of remnants and ambient hydrogen. This is a difficult task, due largely to the relatively low fluxes expected, which approach the limits of sensitivity in the 100 MeV band for past hard gamma-ray experiments such as EGRET.

While this will be addressed by the upcoming GLAST mission, scheduled for launch in 2007, the Imaging Atmospheric Čerenkov Telescope (IACT) technique has focused a large amount of time and energy over the last decade in searching for pion decay signatures in the TeV band. Seminal steps along this path were the announcement of detections of the young remnant SN1006 by CANGAROO (Tanimori et al. 1998), and even younger Cas A by HEGRA (Aharonian et al. 2001) in the northern hemisphere. A second southern remnant, G347.3-0.5 (radio designation, or RX J1713.7-3946 in X-rays), has a claimed detection by the CANGAROO team (Enomoto et al. 2002) in its northwest rim, an asymmetry mirroring the CANGAROO TeV observation of SN1006 (which contrasts its beautifully symmetric radio and X-ray maps: e.g., see Koyama et al. 1995). The RX J1713.7-3946 discovery paper spawned a mini-controversy over whether or not the detection could be interpreted as evidence for hadrons in the remnant. The model interpretation of this remnant forms the focus of this work.

The CANGAROO team offered a hadronic interpretation for the signal they claimed in Enomoto et al. (2002), using particle distributions that would result from linear shock acceleration models. This assessment was disputed in subsequent papers in the literature, in particular Reimer & Pohl (2002) and Butt et al. (2002). These dissenting opinions argued that in order to fit the spectrum published in Enomoto et al. (2002) in the TeV range, the model pion decay flux at 100 MeV energies would be so large that it would far exceed that of the EGRET unidentified source 3EG J1714-3857 lying in the field of view of G347.3-0.5. Whether or not the EGRET source is associated with the remnant is immaterial: it can serve as a putative upper bound, suggesting that an inverse Compton model using cosmic microwave background (CMB) seed photons would be a more viable explanation.

This paper offers additional perspectives on this source, specifically exploring predictions of radiation models that incorporate the physics of non-linear acceleration at remnant shocks. Essentially it updates the careful exploration of Ellison, Slane and Gaensler (2001) that predated the full publication of the CANGAROO data on this source, providing elements of a parameter survey. An update on radio and X-ray observations for this remnant has recently been provided by Lazendic et al. (2004). Yet crucial to multi-wavelength modeling is a recent observational development: the new stereoscopic HESS telescope in Namibia has now detected G347.3-0.5 with an image that nicely matches the X-ray map, albeit with a slightly lower flux and a flatter spectrum from the CANGAROO claim. The HESS results are presented in Aharonian et al. (2004), and complicate the modeling picture considerably, particularly since HESS has not detected SN 1006 (Aharonian et al. 2005), providing upper limits an order of magnitude or more below the CANGAROO data. The model results presented here for G347.3-0.5 will leave the validity of the different TeV data sets to further appraisal by the observational community.

2 Multi-wavelength Models from Non-linear Shocks

Model predictions for supernova remnant emission often invoke linear models of acceleration, where the accelerated particles have no influence on the hydrodynamics of the expanding shock (e.g. Drury, Aharonian & Völk 1994; Gaisser, Protheroe & Stanev 1998; Sturmer et al. 1997; Enomoto, et al. 2002; Reimer & Pohl 2002). Such linear invocations generally suffice to predict X-ray and TeV fluxes to within factors of 3 – 10. Usually, acceleration is considered to take place at the expanding forward shock, though increasingly the importance of acceleration at the reverse shock is being realized (e.g. Decourchelle, Ellison & Ballet 2000; Ellison, Decourchelle & Ballet 2005). Acceleration in strong forward shocks can be very efficient just prior to, or in the early stages of, the Sedov phase, leading to a sizeable fraction of the total energy budget being placed into cosmic rays. Accordingly, energy flux conservation in the shock hydrodynamics is profoundly influenced by the contribution from the highest energy cosmic rays, modifying the shock compression, and hence inducing a non-linear feedback on the acceleration process.

Such non-linear acceleration effects are well-documented in the cosmic ray literature (e.g. see Drury 1983; Jones & Ellison 1991 for reviews). Their key characteristic, a direct consequence of diffusive spatial scales generally being an increasing function of particle momenta, is a deviation from pure power-law behavior in the ion and electron distributions, with an upward curvature indicating more efficient acceleration of the most energetic particles. Such modifications to simpler, linear (test particle) models can influence radiative predictions for comparison with data by factors of 3 – 10 or

more, and therefore become imperative for the theory/observation interface. Detailed models of non-linear acceleration come in different varieties: Monte Carlo simulations have been documented in Ellison & Eichler (1984), Jones & Ellison (1991) and Ellison, Baring & Jones (1996), and analytic/numerical techniques involving diffusion-convection equations have been developed by Kang & Jones (1995), Berezhko, Yelshin & Ksenofontov (1996), Malkov (1997) and Blasi (2002). Extensively-developed applications of these complementary approaches to SNR emission yield similar radiative predictions for similar parameters, so that there is a robustness in the theoretical modeling (e.g. see Baring 2000, for a discussion).

In this paper, a rather compact analytic representation of the non-linear problem developed for ions in Berezhko & Ellison (1999), and extended to treat electrons in Ellison, Berezhko & Baring (2000), is used. This formulation models the non-linear feedback and uses piecewise continuous broken power-laws to approximate the non-thermal distributions. The indices of the power-law segments are determined self-consistently, and the resulting distributions are extremely facile for folding into radiation models for remnants. The reader is referred to Ellison, Berezhko & Baring (2000) for a comprehensive discussion of the acceleration theory, and Ellison, Slane & Gaensler (2001) for a compact presentation on its application to G347.3-0.5.

2.1 *Leptonic Spectral Models*

In the light of the gamma-ray constraints imposed by the EGRET source in the locale of G347.3-0.5 on the sky, it is prudent to focus on inverse Compton models for TeV photon production, following Reimer & Pohl (2002), and many authors in applications to other remnants. The radio to X-ray continuum is modeled with synchrotron emission from a shock-accelerated distribution of electrons, and the same distribution upscatters CMB photons to gamma-ray energies. In such models, spectroscopically, ions go along for the ride, their major role being a power drain for radiative efficiency. Photon production rates are standard calculations, assuming isotropy of electrons, and the reader is referred to Baring et al. (1999), for example, for details.

Ellison, Slane & Gaensler (2001) used the hydrodynamics of a wind-shell interaction to define shock parameters, using these as input into the non-linear acceleration formalism of Ellison, Berezhko & Baring (2000) that was then used to generate photon emission models. Here, the hydrodynamic considerations were not explicitly made, but parameters similar to those of Ellison, Slane & Gaensler (2001; specifically a hybrid of their models A, B and C) were adopted to illustrate the main features. Spectra from the first sample model are illustrated in Fig. 1, together with relevant, published data. This

is a model with a modest upstream field of $B_u = 2\mu\text{G}$ and compression ratio $r_{\text{tot}} = 5$. The field compression of course depends on the shock obliquity, so here we essentially model an almost perpendicular shock, so that $B_d = 10\mu\text{G}$.

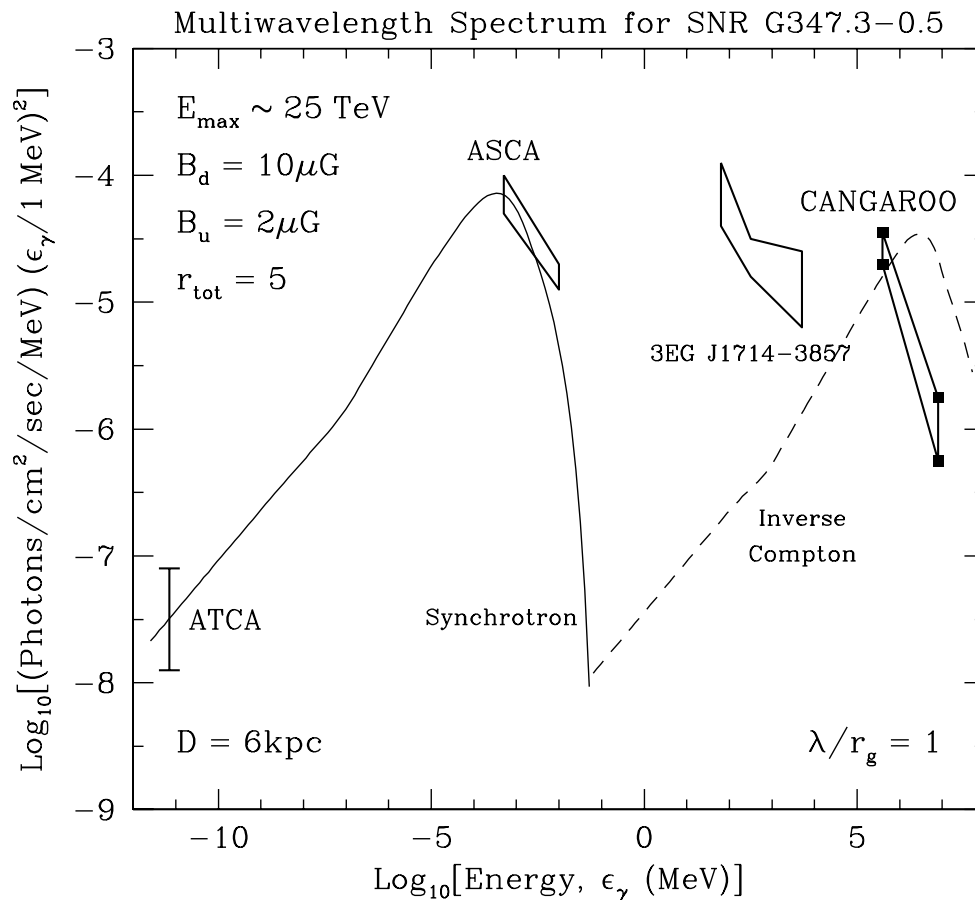


Fig. 1. The multi-wavelength spectra for synchrotron (solid curve) and inverse Compton (dashed) components resulting from a non-linear shock acceleration model of SNR G347.3-0.5 (RX J1713.7-3946). Model/source parameters are as labeled, and are discussed in the text. The observational data consists of 1.36 GHz radio observations by ATCA, a 2–10 keV ASCA X-ray spectrum of the northwest rim (both detailed in Ellison, Slane & Gaensler 2001), a band at $> 300\text{ GeV}$ depicting the steep CANGAROO-II spectrum announced in Enomoto et al. (2002), and a band representing the EGRET unidentified source 3EG J1714-3857, as taken from Reimer & Pohl (2002). Low model densities, $n_p = 0.02\text{ cm}^{-3}$, render the bremsstrahlung and pion decay contributions insignificant at X-ray and TeV energies, respectively.

The upstream particle density is $n_p = 0.02\text{ cm}^{-3}$ for this example, low enough that a pion decay signal would be dominated by the inverse Compton one in the TeV band (see Fig. 3 of Ellison, Slane & Gaensler 2001). For the same reason, the bremsstrahlung contribution would lie far below that of synchrotron emission in the X-ray band, and so is also not exhibited. A source distance of 6 kpc and a remnant age of $t_{\text{SNR}} = 10^4\text{ yrs}$ were adopted,

following the choice of Ellison, Slane & Gaensler (2001) that were based on the contentions of Slane et al. (1999). Debate over the actual distance to SNR G347.3-0.5 will be addressed below.

The spectra in Fig. 1 differ slightly from those exhibited in Fig. 3 of Ellison, Slane & Gaensler (2001), most notably in being a little sharper in the severity of the X-ray and TeV turnovers, and in the prominence of the spectral breaks in the infra-red and the 100 MeV band. Here, the turnovers are structured, broken power-laws, as opposed to the exponential ones opted for in Ellison, Slane & Gaensler (2001). Also, the spectral breaks image the structure of the underlying electron distributions from the simplified, analytic, non-linear acceleration model. Apart from these subtleties, the results are similar, and it is clear that the model predicts a TeV turnover too high to accommodate the steep CANGAROO spectrum.

The global structure of the X-ray and TeV gamma-ray spectral peaks can be quickly understood to be dependent simply on the shock speed, and the strength of the magnetic field. For the parameter regimes chosen to model SNR G347.3-0.5, sufficiently strong B is invoked for the acceleration of electrons (not ions) to be limited by synchrotron cooling. In such cases, the maximum energy of electrons for remnants in the Sedov phase is (for $B > 3\mu\text{G}$, e.g., see Baring et al. 1999):

$$E_{\text{max,e}} \sim \frac{60}{\eta} \left(\frac{B_d}{3\mu\text{G}} \right)^{-1/2} \left(\frac{n_p}{0.01\text{cm}^{-3}} \right)^{-1/5} \left(\frac{t_{\text{SNR}}}{10^4\text{yr}} \right)^{-1/2} \text{TeV} . \quad (1)$$

Here $\eta = \lambda/r_g$ is the ratio of the diffusive mean free path to a particle's gyro-radius, a parameter that couples to diffusive transport across fields and that determines the acceleration rate of electrons and ions. This form guarantees that the X-ray synchrotron turnover energy (i.e., just above the X-ray spectral peak in the νF_ν representation), which is proportional to $E_{\text{max,e}}^2 B_d$, is independent of the field strength, and depends only on the shock speed (e.g. see de Jager et al. 1996, and the discussion in de Jager & Baring 1997) through its dependence on n_p and t_{SNR} .

In contrast, the inverse Compton (IC) peak occurs at an energy $\propto E_{\text{max,e}}^2$ that does scale with the field B_d : higher fields are needed to move the turnover to sub-TeV energies. At the same time, the normalization of the X-ray and TeV peaks is controlled purely by the relative energy densities in the soft CMB photons and the downstream magnetic field, an elementary characteristic (e.g. see Rybicki & Lightman 1979), since the same electrons are emitting in each band. Higher fields enhance the synchrotron component relative to the IC one, i.e. suppress the gamma-rays if the volume filling factor f (here it is around $f = 0.3$) is chosen to fix the radio to X-ray continuum. Hence, it is quickly established that, in the νF_ν representation of Fig. 1, where the y-axis scales

with the emitted power, the X-ray and TeV gamma-ray peaks will be of the same height when $B_d = 3.3\mu\text{G}$. Adjustments in B_d , f and n_p would be needed to try to match the CANGAROO data in Fig. 1. The very recent HESS detection provides additional challenges, as discussed below.

2.2 A Model for Nearby Distances

A crucial ingredient in the model presented in Fig. 1 is the assumption that the source is 6 kpc distant. Koyama et al. (1997) obtained a distance estimate of $D = 1\text{ kpc}$ based on the column density inferred from soft X-ray absorption in ASCA data, when compared to the Galactic Center direction absorption characteristics. This contention has recently been supported by XMM observations (Cassam-Chenaï et al. 2004) and also evidence for molecular cloud material at 1 kpc (Fukui et al. 2003). Clearly, for the observed expansion rate, the age of the remnant is therefore uncertain by a factor of 6 (though it would still be inferred to be in the Sedov phase), and so also is the inferred mean density in the remnant, because of the relationship between density n_p and distance D for fixed source synchrotron flux: $F \propto n_p D = \text{constant}$. Slane et al. (1999) favored the larger 6 kpc value, principally because they observed that CO intensity mapping suggested a projected association of the remnant with three molecular clouds that appeared to have CO and HI column densities matching the X-ray values. The radial velocities of these clouds indicates a minimum distance of $D = 6\text{ kpc}$ when folded into a galactic rotation model. This reasoning obviously depends on the validity of the association.

The debate in the literature over this distance has not been conclusively resolved. Accordingly, presenting a model for a $D = 1\text{ kpc}$ case is clearly motivated. This translates to assuming a density around $n_p \sim 0.2\text{ cm}^{-3}$, for which we will not treat bremsstrahlung or line emission here. From Eq. (1), this change in density would force $E_{\text{max,e}}$ lower so as to move the synchrotron peak below the X-ray band. Adjusting B_d upwards is to no avail, since the synchrotron peak energy is independent of field strength in this cooling-dominated domain. Hence to fit the ASCA continuum, lower fields are desirable to emerge from cooling-limited acceleration phase space, and thereby render $E_{\text{max,e}}$ sensitive to the choice of B_d . For fields $B \lesssim 3\mu\text{G}$, synchrotron cooling is generally insignificant, and the maximum energy of accelerated electrons is controlled by the spatial scale of the remnant (e.g. Baring et al. 1999):

$$E_{\text{max,e}} \sim \frac{170}{\eta} \left(\frac{B_u}{3\mu\text{G}} \right) \left(\frac{n_p}{\text{cm}^{-3}} \right)^{-1/5} \left(\frac{t_{\text{SNR}}}{10^4\text{yr}} \right)^{-1/2} \text{TeV} . \quad (2)$$

For the higher density and younger age dictated by choosing $D = 1\text{ kpc}$, a field of $B_d = 2\mu\text{G}$ yields a synchrotron νF_ν peak in the classical X-ray band.

A model spectrum corresponding to this case is depicted in Fig. 2. The compression ratio of $r_{tot} = 6.4$ was slightly higher than in the first example (due in part to a higher electron-to-proton abundance ratio and a higher value of $E_{\max,e}$ that spawns increased losses in the non-linear acceleration model), and again represented B_d/B_u as in a quasi-perpendicular shock. The maximum electron (and proton) energy was 60 TeV in this case, markedly higher than in Fig. 1. Consequently, the inverse Compton νF_ν peak moves to above 10 TeV, a gross mismatch to the putative CANGAROO points. The flux in the IC peak now exceeds that for the X-ray synchrotron peak, since now the magnetic field energy density is inferior to that of the cosmic microwave background.

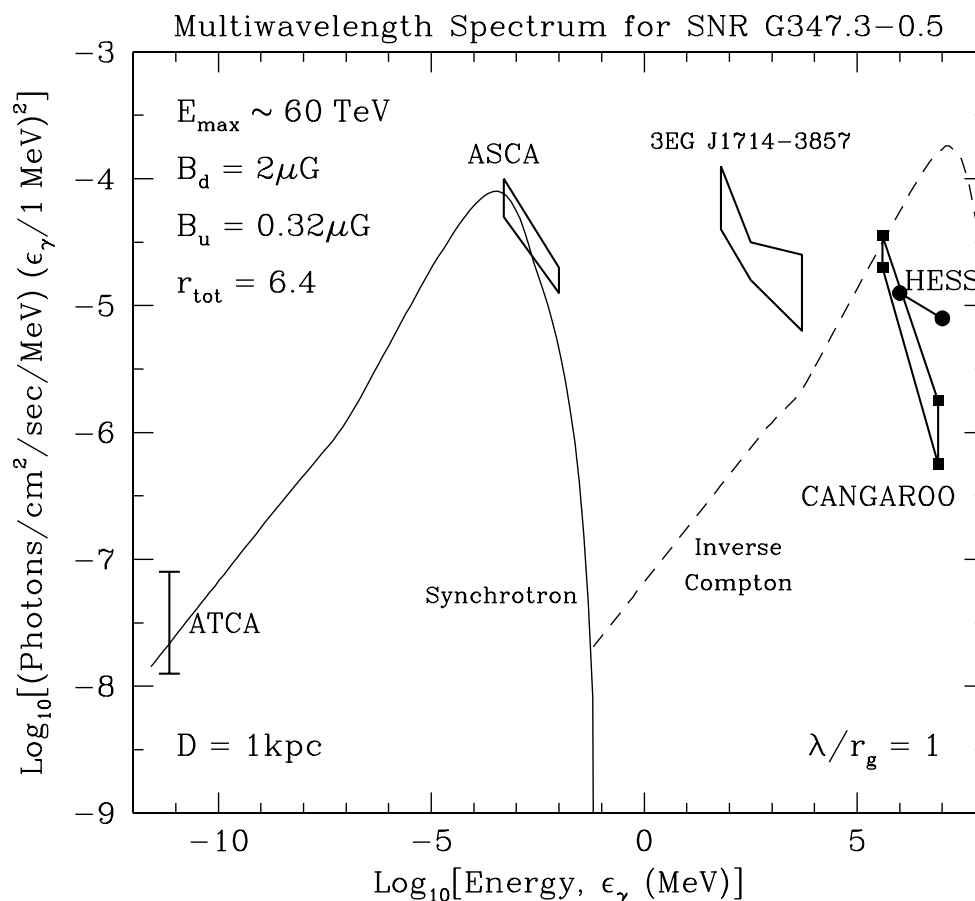


Fig. 2. The multi-wavelength model spectrum resulting from a non-linear shock acceleration model of SNR G347.3-0.5 (RX J1713.7-3946) for an assumed distance of $D = 1$ kpc, following the proposition of Koyama et al. (1997). The two spectral components are synchrotron emission (solid curve) and inverse Compton scattering (dashed). Model and source parameters are as labeled. The observational data are as in Fig. 1, with the addition of the $E^{-2.2}$ spectrum for the TeV detection recently announced by the HESS telescope team (Aharonian et al. 2004); see text for a discussion on normalization.

Also marked on the Figure is the spectrum announced by the HESS team in Aharonian et al. (2004). This spectrum is very different from the CANGAROO one. Not only is it flatter ($dn/dE \propto E^{-2.2}$ as opposed to $dn/dE \propto E^{-2.8}$), it possesses slightly higher overall flux. The HESS result is integrated over the entire remnant, and therefore differs in normalization from the CANGAROO result, which was for the northwest rim portion only. For the purposes of the model comparison, the HESS spectrum from just this confined portion of the rim is somewhat lower than the CANGAROO data, reflecting the sensitive nature of the HESS telescope array. It is noteworthy that the HESS detection is spatially resolved, mirroring the ASCA sky map more closely due to its improved angular resolution. Clearly the HESS results are at odds with the CANGAROO data, a topical issue that will be the subject of discussion by the TeV astronomy community in the coming years. Moreover, the HESS data are just as difficult to reconcile with the model spectrum, as depicted.

This multiwavelength modeling could be viewed as another argument against adopting $D = 1$ kpc for the distance to SNR G347.3-0.5. However, it should be noted that the models were restricted to the Bohm diffusion limit $\eta = \lambda/r_g = 1$, where a particle's diffusive scale is the smallest possible, i.e. its gyroradius, corresponding to strong field turbulence. Therefore, less turbulent shock environments can increase the diffusive scale, thereby reducing the acceleration rate and lowering $E_{max,e}$ (see Eqs. (1) and (2)) without necessarily altering other environmental parameters such as B_d and n_p . Modifications along these lines can, with a slight adjustment upwards in field strength, approximately match the CANGAROO data in Fig. 2, but might have greater difficulty in accommodating the portion of the HESS signal coming from the northwest rim, which would require higher fields in order to reduce the inverse Compton to synchrotron ratio at their respective peaks.

2.3 Hadronic Models?

Having explored the case for purely leptonic models, it is worth noting that hadronic models for the generation of gamma-rays are in principal tenable for SNR G347.3-0.5, though not in the simplest form envisaged by Enomoto et al. (2002) in their original claim. The objections of Reimer & Pohl (2002) and Butt et al. (2002) still stand. However the complex environment of the remnant admits the possibility that pions can be created using molecular cloud nucleons as targets for the energetic cosmic rays, and these would be somewhat remote from the expanding outer shell of SNR G347.3-0.5. Such a departure from a one-zone scenario is quite reasonable in these circumstances.

A spatial separation of accelerator and target alters the expected spectrum for pion decay emission. Since the diffusive scale of the higher energy ions is

larger than that for the low energy ones that contribute to the π^0 decay peak at 67 MeV (e.g. see Jones & Ellison 1991; Baring et al. 1999; Berezhko & Ellison 1999, for a discussion of such diffusion lengths), the latter ions have great difficulty in convecting far upstream of the shocked shell. Consequently, the pion signal would be strongly suppressed near 67 MeV in this scenario, as would all such emission from particles whose energies correspond to diffusive scales less than the distance between the shell and the target cloud. This would skew the π^0 decay spectrum to render it peaked near the TeV band in the νF_ν representation, thereby evading the EGRET source bounds.

Clearly, for this geometrical separation to have a significant impact on the pion decay continuum, the distance between remnant shell and target molecular cloud must be at least a sizable fraction of the radius of the remnant. Such a model is not unduly contrived, but does require additional parameters relating to spatial scales and turbulence (i.e. $\eta = \lambda/r_g$) that are poorly constrained by observational data, particularly given the impact of line-of-sight ambiguities to the environmental geometry. Furthermore, these parameters might well have to vary significantly across the remnant in order to reconcile the molecular cloud sky geometries with the X-ray and TeV emission morphologies. Finally, it might prove difficult to distinguish this pion decay scenario spectroscopically from inverse Compton emission, given that both would be extremely flat and statistics-limited somewhat below the TeV peak.

3 Conclusions

In closing, two multi-wavelength models are presented here for broadband emission in SNR G347.3-0.5, using fundamental characteristics of non-linear shock acceleration as their basis. This offering is not designed to find the “perfect” model fit, but rather to represent samples from an array of possibilities that indicate how such multi-wavelength approaches can constrain model parameter space. While the examples are focused on an inverse Compton origin of TeV emission, which is the preferred interpretation in a low density remnant environment, it is also emphasized that hadronic models with pion decay emission in the TeV band are not presently ruled out. Using nucleonic targets in proximate molecular clouds that are distinct from the remnant shell can potentially generate acceptable model fits to TeV datasets.

The study of this remnant is presently burdened with the controversy concerning the TeV data, an issue also for SN 1006, which has so far not been detected by HESS (Aharonian et al. 2005). The contradictory results for SNR G347.3-0.5 between CANGAROO and HESS obviously need to be resolved in order to propel theoretical understanding at a more rapid pace. This is a challenge that the TeV community met in the case of the Crab nebula, and

northern hemisphere blazars, that established the branch of TeV astronomy on a firm basis. For supernova remnants, this bridge has yet to be crossed. Anticipating watershed results from the increasing number of IACTs to be in operation in both hemispheres over the next few years, such a development will hopefully be around the corner.

4 References

- Aharonian, F., Akhperjanian, A. G., Barrio, J., et al. Evidence for TeV gamma ray emission from Cassiopeia A. *Astron. Astrophys.* 370, 112–120. 2001.
- Aharonian, F., Akhperjanian, A. G., Aye, K.-M., et al. High-energy particle acceleration in the shell of a supernova remnant. *Nature* 432, 75–77. 2004.
- Aharonian, F., Akhperjanian, A. G., Aye, K.-M., et al. Upper limits to the SN1006 multi-TeV gamma-ray flux from H.E.S.S. observations. *Astron. Astrophys.* in press. 2005.
- Baring, M. G., Ellison, D. C., Reynolds, S. P., et al. Radio to Gamma-Ray Emission from Shell-Type Supernova Remnants: Predictions from Nonlinear Shock Acceleration Models. *ApJ* 513, 311–338. 1999.
- Baring, M. G. Modelling Hard Gamma-Ray Emission From Supernova Remnants. in *GeV–TeV Gamma-Ray Astrophysics Workshop*, ed. B. L. Dingus, M. H. Salamon, & D. B. Kieda (AIP Conf. Proc. 515, New York), pp. 173–182. [[astro-ph/9911060](#)] 2000.
- Berezhko, E. G., Ellison, D. C. A Simple Model of Nonlinear Diffusive Shock Acceleration. *ApJ* 526, 385–399. 1999.
- Berezhko, E. G., Yelshin, V., Ksenofontov, L. T. Cosmic Ray Acceleration in Supernova Remnants. *Sov. Phys. JETP* 82, 1–21. 1996.
- Blasi, P. A semi-analytical approach to non-linear shock acceleration. *Astroparticle Phys.* 16, 429–439. 2002.
- Butt, Y. M., Torres, D. F., Romero, G. E., et al. Supernova-Remnant Origin of Cosmic Rays? *Nature* 418, 499–499. 2002.
- Cassam-Chenaï, G., Decourchelle, A., Ballet, J., et al. XMM-Newton observations of the supernova remnant RX J1713.7-3946 and its central source observations of SNR RX J1713.7-3946. *Astron. Astrophys.* 427, 199–216. 2004.
- Decourchelle, A., Ellison, D. C., Ballet, J. Thermal X-Ray Emission and Cosmic-Ray Production in Young Supernova Remnants. *ApJ* 543, L57–L60. 2000.
- de Jager, O. C., Baring, M. G. Supernova Remnants and Plerions in the Compton Gamma-Ray Observatory Era. in *Proc. 4th Compton Symposium*, ed. Dermer, C. D. & Kurfess, J. D. (AIP Conf. Proc. 410, New York), pp. 171–180. [[astro-ph/9711212](#)] 1997.
- de Jager, O. C., Harding, A. K., Michelson, P. F., et al. Gamma-Ray Observations of the Crab Nebula: A Study of the Synchro-Compton Spectrum.

- ApJ 457, 253–266. 1996.
- Drury, L. O’C. An Introduction to the Theory of Diffusive Shock Acceleration of Energetic Particles in Tenuous Plasmas. Rep. Prog. Phys. 46, 973–1028. 1983.
- Drury, L. O’C., Aharonian, F. A., Völk, H. J. The gamma-ray visibility of supernova remnants. A test of cosmic ray origin. Astron. Astrophys. 287, 959–971. 1994.
- Ellison, D. C., Baring, M. G., Jones, F. C. Nonlinear Particle Acceleration in Oblique Shocks. ApJ 473, 1029–1050. 1996.
- Ellison, D. C., Berezhko, E. G., Baring, M. G. Nonlinear Shock Acceleration and Photon Emission in Supernova Remnants. ApJ 540, 292–307. 2000.
- Ellison, D. C., Decourchelle, A., Ballet, J. Nonlinear particle acceleration at reverse shocks in supernova remnants. Astron. Astrophys. 429, 569–580. 2005.
- Ellison, D. C., Eichler, D. Monte Carlo shock-like solutions to the Boltzmann equation with collective scattering. ApJ 286, 691–701. 1984.
- Ellison, D. C., Slane, P. O., Gaensler, B. M. Broadband Observations and Modeling of the Shell-Type Supernova Remnant G347.3-0.5. ApJ 563, 191–201. 2001.
- Enomoto, R., Tanimori, T., Naito, T., et al. The acceleration of cosmic-ray protons in the supernova remnant RX J1713.7-3946. Nature 416, 823–826. 2002.
- Fukui, Y., Moriguchi, Y., Tamura, K., et al. Discovery of Interacting Molecular Gas toward the TeV Gamma-Ray Peak of the SNR G 347.3-0.5. Pub. Astron. Soc. Japan 55, L61–L64. 2003.
- Gaisser, T. K., Protheroe, R. J., Stanev, T. Gamma-Ray Production in Supernova Remnants ApJ 492, 219–227. 1998.
- Jones, F. C., Ellison, D. C. The plasma physics of shock acceleration. Space Sci. Rev. 58, 259–346. 1991.
- Kang, H., Jones, T. W. Diffusive Shock Acceleration Simulations: Comparison with Particle Methods and Bow Shock Measurements. ApJ 447, 944–961. 1995.
- Koyama, K., Petre, R., Gotthelf, E. V., et al. Evidence for Shock Acceleration of High-Energy Electrons in the Supernova Remnant SN:1006. Nature 378, 255–257. 1995.
- Koyama, K., Kinugasa, K., Matsuzaki, K., et al. Discovery of Non-Thermal X-Rays from the Northwest Shell of the New SNR RX J1713.7-3946: The Second SN 1006? Pub. Astron. Soc. Japan 49, L7–L11. 1997.
- Lazendic, J. S., Slane, P. O., Gaensler, B. M., et al. A High-Resolution Study of Nonthermal Radio and X-Ray Emission from Supernova Remnant G347.3-0.5. ApJ 602, 271–285. 2004.
- Malkov, M. A. Analytic Solution for Nonlinear Shock Acceleration in the Bohm Limit. ApJ 485, 638–654. 1997.
- Reimer, O., Pohl, M. No evidence yet for hadronic TeV gamma-ray emission from SNR RX J1713.7-3946. Astron. Astrophys. 390, L43–L46. 2002.

- Rybicki, G. B., Lightman, A. P. Radiative Processes in Astrophysics (Wiley, New York) 1979.
- Slane, P. O., Gaensler, B. M., Dame, T. M., et al. Nonthermal X-Ray Emission from the Shell-Type Supernova Remnant G347.3-0.5 ApJ 525, 357–367. 1999.
- Sturner, S. J., Skibo, J. G., Dermer, C. D., Mattox, J. R. Temporal Evolution of Nonthermal Spectra from Supernova Remnants. ApJ 490, 619–632. 1997.
- Tanimori, T., Hayami, Y., Kamei, S., et al. Discovery of TeV Gamma Rays from SN 1006: Further Evidence for the Supernova Remnant Origin of Cosmic Rays. ApJ 497, L25–L28. 1998.